

# Continuous broadband tuning of an electron-beam-pumped XeF ( $C \rightarrow A$ ) laser

J. Liegel,<sup>a)</sup> F. K. Tittel, and W. L. Wilson, Jr.

Electrical Engineering Department, and Rice Quantum Institute, Rice University, Houston, Texas 77001

G. Marowsky

Max-Planck Institut für Biophysikalische Chemie, Abteilung Laserphysik, D-3400 Göttingen, Federal Republic of West Germany

(Received 13 May 1981; accepted for publication 9 June 1981)

Wide-band tuning of a XeF ( $C \rightarrow A$ ) excimer laser pumped with a longitudinal electron beam was demonstrated from 455 to 529 nm. The spectral linewidth of the laser emission was  $\sim 5$  nm when a prism was used as a wavelength selecting element, and narrowed to  $\sim 1$  nm when the prism was replaced by a diffraction grating.

PACS numbers: 42.55.Hq, 42.60.By, 41.80.Dd

The development of a broadly tunable excimer laser source by exploiting bound-free transitions of diatomic and triatomic rare-gas halides is of considerable interest in many applications, such as spectroscopy and laser-induced chemistry. Wavelength tuning of an excimer was first demonstrated with the Xe<sub>2</sub> laser centered at 172 nm.<sup>1</sup> Spectral tuning ranges of 4 nm for an Ar<sub>2</sub> laser<sup>2</sup> and  $\sim 2$  nm for ArF, KrF, XeCl, and XeF (Refs. 3 and 4) have been reported. Recently, laser action has been observed in XeF ( $C \rightarrow A$ ) (Refs. 5–8), Xe<sub>2</sub>Cl (Ref. 9), and Kr<sub>2</sub>F (Ref. 10) excimers, which are capable of broad wavelength tunability in the blue-green region of the spectrum. Broad spectral tuning was first demonstrated for a photolytically pumped XeF ( $C \rightarrow A$ ) laser.<sup>11</sup> This letter describes the characteristics of an electron-beam-pumped XeF ( $C \rightarrow A$ ) laser which can be continuously tuned over a range of 74 nm from 455 to 529 nm with a minimum spectral linewidth of 1 nm. The laser is excited longitudinally by the electron beam, and operates on an electronic transition involving a bound ionic excited  $C$  state and a repulsive  $A$  state on the long-wavelength side of the bound-weakly bound  $B \rightarrow X$  transition at 351 and 353 nm.<sup>12</sup>

The experimental apparatus shown in Fig. 1 consists of an electron beam generator, a laser cell, and diagnostic instrumentation for optical and electrical measurements. In this work we employ a longitudinal pump geometry rather than transverse<sup>5,9</sup> or radial electron beam excitation.<sup>1,2</sup> Electrons produced by the accelerator are magnetically guided into the laser cell. This permits efficient electron beam energy deposition in the rare-gas-halide mixtures and a much longer effective gain length which is needed in tuning experiments that involve inherently low-gain broadband excimers.<sup>13</sup> Insertion losses of the wavelength selective elements must not exceed the net gain of the excimer medium. The design of the laser cell is based on the " $\lambda$ " geometry developed at Sandia Laboratories.<sup>14</sup> A simpler "head-on" configuration has been described in Ref. 15. However, this design requires the electron beam to pass through one of the laser cavity reflectors. Electron beam pulses (10 kA, 1 MeV, 10 ns pulse width) from a Physics International Pulserad 110 accelerator are injected into the laser cell through a 50- $\mu$ m-thick titanium foil, which serves both as the anode of the

field-emission diode as well as the pressure barrier between the diode and the laser gas mixture. Magnetic confinement of the electron beam by three axial magnetic field coils is used to both guide the electrons, and minimize loss by beam spreading as it passes down the laser cell (Fig. 1). The laser cell consists of a 5-cm-diam, 1-m-long thin-walled (0.08 cm) stainless-steel tube with an active length of 80 cm. Several criteria determine the choice of dimensions, such as effective electron beam energy deposition at the highest operating pressure. Furthermore the magnetic field must penetrate the metallic cell wall in a time that is short compared with the magnetic pulse duration. Optimum triggering of the Marx generator relative to the magnetic field pulsed power supply is achieved using the adjustable delay of an HP model 214B pulse generator. The electron beam pump pulse is produced when the magnetic field of the main solenoid  $B_s$  reaches its maximum of 6 kG with a delay of  $\sim 1$  ms, as shown in Fig. 2(a). An electron beam turning coil is aligned in such a way that the beam is centered in the laser cell. A set of Helmholtz coils at the end of the cell deflects the remaining electrons from the laser optics. The electron beam profile was evaluated using diazochrome foils, and the electron energy coupled into the cell was measured with a graphite disk calorimeter. In the main magnetic field region of the tube, immediately following the bend, the beam energy was measured to be 10 J, with a spatial FWHM of 27 mm in 2 atm of argon buffer gas.

In order to minimize insertion losses, intracell laser mirrors and dispersive elements are employed, which can be conveniently aligned with metal bellows mounts. The output coupler was typically a concave reflector ( $r = 10$  m,

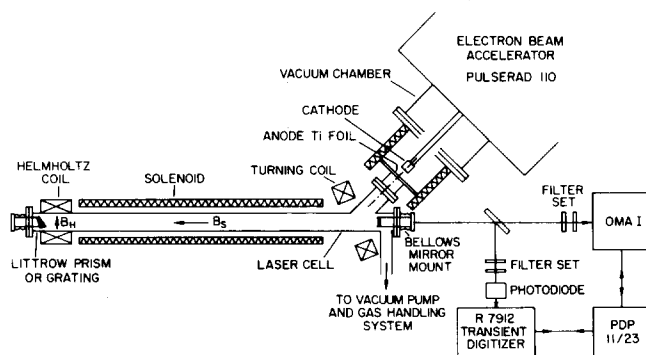


FIG. 1. Schematic diagram of the experimental arrangement.

<sup>a)</sup>Present address: Physikalisches Institut, University of Würzburg, Federal Republic of West Germany.

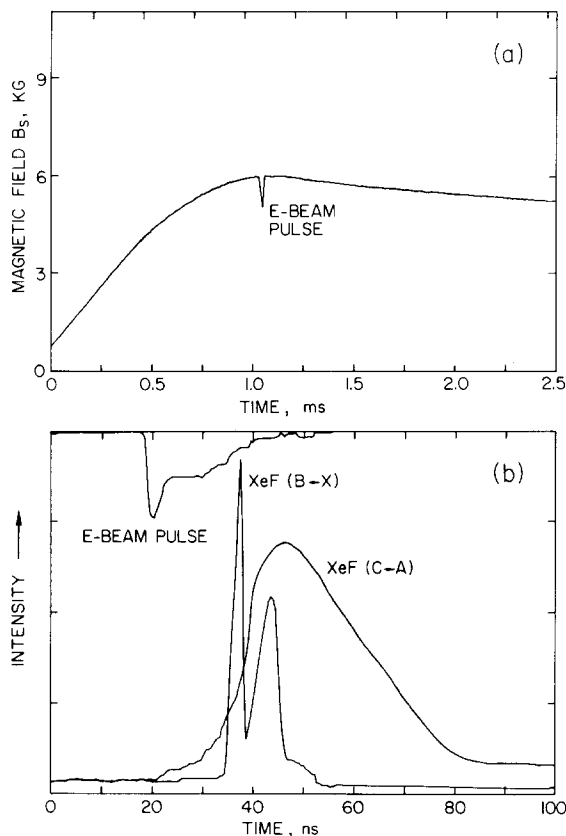


FIG. 2. Temporal characteristics of (a) the magnetic field, and (b) the laser emission for XeF( $B \rightarrow X$ ) transition at 351 and 353 nm and the prism-tuned XeF( $C \rightarrow A$ ) pulse at 488 nm for a mixture of 8-Torr Xe, 3-Torr  $\text{NF}_3$ , and 2-atm Ar. The electron beam current pulse as monitored by a Faraday cup probe located 5 cm from the laser cell bend is also depicted for reference.

$T = 5\%$ ). The dispersive optical element was either a Littrow prism reflector ( $R > 99\%$ ) made of a high-dispersion glass (Schott SF59) or a diffraction grating (600 lines/mm,  $R \approx 77\%$  at 490 nm). The cell can also be fitted with Brewster windows, for use with external optics.

Time-resolved fluorescence and laser signals were monitored with an ITT F-4000 S-5 vacuum photodiode and a Tektronix R7912 Transient Digitizer. Spectrally resolved signals were obtained with a PAR OMA-1 optical multi-channel analyzer. A wide-band interference filter centered at 500 nm and a Corning 3-73 color filter ensured good spectral rejection of the much stronger  $B \rightarrow X$  emission at 351 and 353 nm. All of the temporal and spectral data were stored and reduced with a DEC PDP 11/23 minicomputer system.

Fluorescence measurements were used to determine the optimum gas composition, which was found to be 3-Torr  $\text{NF}_3$ , 8-Torr Xe, and 2-atm Ar. Time-integrated fluorescence and laser spectra are shown in Fig. 3 for an untuned laser that used a concave mirror ( $r = 10$  m and  $R \approx 99\%$  at 490 nm) as an end reflector. The spectral bandwidth narrowed from 50 nm for fluorescence to 30 nm when lasing is as depicted in Fig. 3(a) and 3(b). The center wavelength of the stimulated emission also shifted about 15 nm owing to the spectral characteristics of the laser optics used. Atomic absorption features arising from xenon metastable transitions<sup>8,13</sup> are visible in the fluorescence spectrum and greatly enhanced in the laser spectrum. The output laser power was

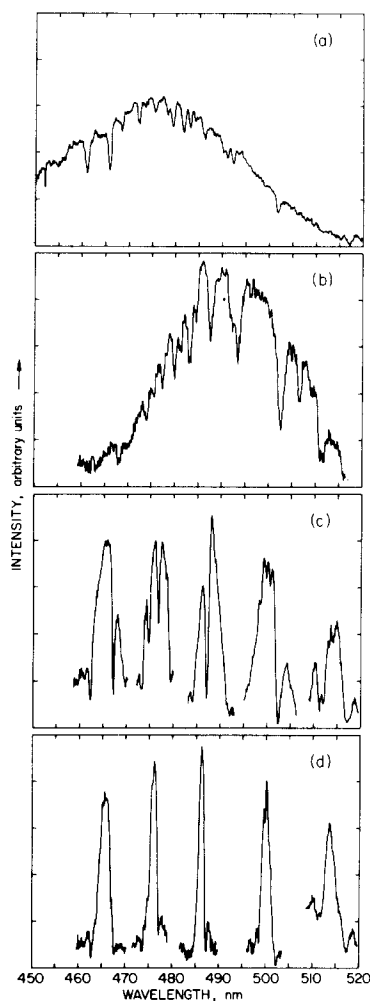


FIG. 3. Time integrated spectra of the XeF( $C \rightarrow A$ ) emission showing (a) fluorescence, (b) laser emission with an untuned cavity, (c) laser emission with the prism tuner, and (d) laser emission with the grating tuner. The gas mixture was 8-Torr Xe, 3-Torr  $\text{NF}_3$  and 2-atm Ar.

measured to be  $\sim 30 \text{ kW/cm}^2$ . When the back mirror is replaced by a Littrow prism, the spectral bandwidth of the laser narrows to 5 nm [Fig. 3(c)]. The cavity was conveniently aligned and calibrated using ten different lines of an  $\text{Ar}^+$  laser tuned from 454.5 to 528.7 nm. XeF( $C \rightarrow A$ ) laser action is observed throughout this region, with the maximum output power ( $1 \text{ kW/cm}^2$ ) occurring at 488 nm. The power decreases by 10% at 455 and 529 nm. When the prism tuner is replaced by a diffraction grating, even narrower spectral linewidths of 1–2 nm are observed [Fig. 3(d)]. Stimulated emission could now be tuned off the strong atomic absorption lines visible in Fig. 3(a)–(c). The halogen donor  $\text{NF}_3$  does not attack the grating, as originally feared. Broader linewidth and lower laser output powers resulted when using the grating external to the laser cell.

Competition between the XeF( $B \rightarrow X$ ) and XeF( $C \rightarrow A$ ) emission is considerably more severe for longitudinal pumping than with transverse electron excitation. Amplified spontaneous emission occurs on the  $B \rightarrow X$  transition corresponding to two vibrational ground-state states at 351 and 353 nm. The temporal behavior of the XeF( $B \rightarrow X$ ) pulses is shown in Fig. 2(b). Two pulses of 3-ns duration occur immediately after the  $e$ -beam excitation pulse. Owing to the favorable Franck–Condon factor, lasing is expected to begin at the 351.1-nm transition ( $v' = 0 \rightarrow v'' = 2, v' = 1 \rightarrow v'' = 4$ ) with subsequent shifting to the 352-nm transition

( $v' = 0 \rightarrow v'' = 3$ ).<sup>16</sup> The XeF ( $C \rightarrow A$ ) laser pulse occurs with a typical delay of 30 ns. The temporal width of the laser pulse appears to vary considerably from as long as 80 ns to as short as 20 ns, depending on the optical resonator geometry.

In summary, we have demonstrated broadband tuning and spectral narrowing for the XeF ( $C \rightarrow A$ ) laser in the range from 455 to 529 nm. Either a prism or a grating could be used as the dispersive element. To improve the output power of this laser, it will be necessary to suppress the strong XeF ( $B \rightarrow X$ ) transition. This can be achieved by going to higher Ar buffer gas pressures. Since 1-MeV electrons do not have sufficient range to penetrate more than about 2 atm of argon for a distance of 1 m, a shorter cell geometry will be required for higher pressure studies. Construction of a 30-cm head-on cell is in progress. The cell will employ dielectrically coated Cervit or sapphire plates (0.3 mm thick). These mirrors have been shown to be able to withstand the electron beam for more than 25 shots and are transparent to the electron beam pulse.

We would like to thank G. Zenhua and R. Williams for their experimental assistance, and M. C. Smayling for his helpful advice on this project. We are also grateful to R. A. Klein and his colleagues for supplying details of the Sandia HF laser system. We also thank H. C. Kirbie for helping to design the pulsed magnetic field power supply. This work was supported by the Office of Naval Research, the Robert

Welch Foundation, and the National Science Foundation.

- <sup>1</sup>D. J. Bradley, D. R. Hull, M. H. R. Hutchinson, and M. W. McGeoch, *Opt. Commun.* **14**, 1 (1975).  
<sup>2</sup>W. G. Wrobel, H. Rohr, and K. H. Steuer, *Appl. Phys. Lett.* **36**, 113 (1980).  
<sup>3</sup>T. R. Loree, K. B. Butterfield, and D. L. Baker, *Appl. Phys. Lett.* **33**, 171 (1978).  
<sup>4</sup>R. T. Hawkins, H. Egger, J. Bokor, and C. K. Rhodes, *Appl. Phys. Lett.* **36**, 391 (1980).  
<sup>5</sup>W. E. Ernst and F. K. Tittel, *Appl. Phys. Lett.* **35**, 36 (1979).  
<sup>6</sup>W. K. Bischel, H. H. Nakano, D. J. Eckstrom, R. M. Hill, D. L. Huestis, and D. C. Lorents, *Appl. Phys. Lett.* **34**, 565 (1979).  
<sup>7</sup>R. Burnham, *Appl. Phys. Lett.* **35**, 48 (1979).  
<sup>8</sup>C. H. Fisher, R. E. Center, G. J. Mullaney, and J. P. McDaniel, *Appl. Phys. Lett.* **35**, 26 (1979).  
<sup>9</sup>F. K. Tittel, W. L. Wilson, R. E. Stickel, G. Marowsky, and W. E. Ernst, *Appl. Phys. Lett.* **36**, 405 (1980).  
<sup>10</sup>F. K. Tittel, G. Marowsky, M. C. Smayling, and W. L. Wilson, *Appl. Phys. Lett.* **36**, 381 (1980).  
<sup>11</sup>W. K. Bischel, D. J. Eckstrom, D. L. Huestis, and D. C. Lorents, *Lasers '79*, Orlando, Florida, 1979 (unpublished).  
<sup>12</sup>*Excimer Lasers*, edited by C. K. Rhodes (Springer, Berlin, 1979).  
<sup>13</sup>F. K. Tittel, W. L. Wilson, M. C. Smayling, and G. Marowsky, *IEEE J. Quantum Electronics* (to be published).  
<sup>14</sup>R. A. Klein, " $\lambda$ -3, Sandia's 100-J HF Laser System," Sandia Report SAND 79-1659, (1979).  
<sup>15</sup>R. Sauerbrey and H. Langhoff, *Appl. Phys.* **22**, 399 (1980).  
<sup>16</sup>S. F. Fulghum, M. S. Feld, and A. Javan, *IEEE J. Quantum Electron.* **QE-16**, 815 (1980).

## ZnI ( $B \rightarrow X$ ) laser: 600–604 nm

A. W. McCown and J. G. Eden

*Electrical Engineering Research Laboratory, Department of Electrical Engineering, University of Illinois at Urbana-Champaign, Urbana, Illinois 61801*

(Received 15 May 1981; accepted for publication 2 June 1981)

Lasing on several transitions of the  $B^2\Sigma \rightarrow X^2\Sigma$  band of zinc-iodide (ZnI) with wavelengths ranging from 600 to 604 nm has been demonstrated. Pumped by the dissociative excitation of ZnI<sub>2</sub> (using an ArF excimer laser), this laser exhibits many of the optical and chemical properties of the HgBr<sub>2</sub> blue-green dissociation laser.

PACS numbers: 42.55.Hq, 33.80.Gj

The peak emission wavelengths for the  $B \rightarrow X$  bands of the group IIB metal-halide diatomic radicals (HgCl, ZnBr, etc.) extend from the violet ( $\lambda \sim 440$  nm: HgI) to the near-infrared ( $\lambda \sim 800$ – $830$  nm: zinc and cadmium bromides). Previously, lasing has been reported for the mercury halides HgCl, HgBr, and HgI. Pumping of the upper laser level was accomplished by ultraviolet photodissociation of the HgX<sub>2</sub> salts ( $X = \text{Cl, Br, or I}$ ),<sup>1–3</sup> dissociative excitation of these same dihalide molecules in a fast transverse discharge<sup>4,5</sup> or by relativistic electron beam irradiation of gas mixtures containing Hg and the desired halogen donor.<sup>6–8</sup> As pointed out by Schimitschek and Celto,<sup>4</sup> the first two pumping methods

(photo or electrical dissociation of a metal salt) have an advantage over the third in that they involve a cyclical production scheme for the excited species. That is, the HgX<sub>2</sub> molecules reform following lasing. These and other attractive features of the Hg halides (such as the Franck–Condon shift between the  $B$  and  $X$  states) are also embodied by the zinc- and cadmium-halide diatomic radicals.

The first observation of lasing in the visible from a zinc-halide diatomic molecule is reported in this letter. Stimulated emission on the  $B^2\Sigma \rightarrow X^2\Sigma$  band of ZnI has been obtained in the wavelength interval  $600 \leq \lambda \leq 604$  nm by photodissociating ZnI<sub>2</sub> in the presence of a buffer gas (Ar or Ne) using